Proceedings of the 8th IEEE Mediterranean Conference
on Control and Automation (MED 2000)
Rio, Patras, GREECE 17-19 July, 2000

Fuzzy Neural Network–based Internal Model Control for DC– Motor Micromaneuvering

Jamahl W. Overstreet and Anthony Tzes

Abstract— **The development of a Fuzzy Neural Network (FNN)–based Internal Model Control (IMC)–scheme and its application to a dc–motor micromaneuvering system is addressed in this article. The FNN is tuned in an off–line manner in order to cancel the motor's inherent nonlinear friction term. The resulting FNN is used in the feedback path, augmented by a primitive linear time–invariant controller in the forward path. The adjustment of the linear controller's parameters relies on the IMC–framework based on the premise that the system's nonlinearities have benn canceled by the FNN. The suggested controller–structure is tested in experimental studies at a dc–motor testbed to investigate its efficiency.**

Keywords— **Fuzzy neural network, Friction compensation, DC–motor control.**

I. Introduction

In this article, the development and testing of a nonlinear internal model controller for micro-maneuvering purposes of a dc– motor is investigated. The reason behind the selection of an IMC– structure is due to its robustness against plant uncertainty and disturbance rejection. The classical IMC–theory [1–7] was primarily developed for linear plants and generates linear controllers. However, the dc–motor system has certain nonlinearities stemming from the Coulomb and static friction properties. Inhere, the proposed hybrid nonlinear IMC is optimized to account for compensation against additive nonlinearities in the underlying linear model of the dc–motor system.

The suggested IMC–structure, shown in Figure 1, consists of the following components: 1) a module for modeling the nonlinear dc–motor system; this module is also used to cancel the nonlinear components of the system, and 2) a feedback controller module to enhance the system's closed–loop performance.

Towards the identification problem for the nonlinear dc–motor system, a FNN–identifier was developed. The generated FNN–model is subsequently used to cancel the effects of the nonlinear friction dynamics. A rather primitive IMC–based proportional controller is utilized in the feedback module, primarily because of its simplicity towards its implementation. A FNN [8, 9] is a combination of using a fuzzy logic expert system [10–15] with an auto–tuned artificial neural network [5, 8, 16–18].

The suggested nonlinear IMC–framework is applied to a dc–motor setup in order to investigate its efficiency. The FNN–based identifier identifies and compensates the nonlinear friction dynamics while the feedback controller is used to improve the system's performance.

J.Overstreet is with Polytechnic University, Mechanical Engineering Department, Six Metrotech Center, Brooklyn, NY 11201, U.S.A.
A.Tzes is with University of Patras, Electrical & Computer Engineering Department, Rio 26500, GREECE, E-mail: tzes@ee.upatras.gr

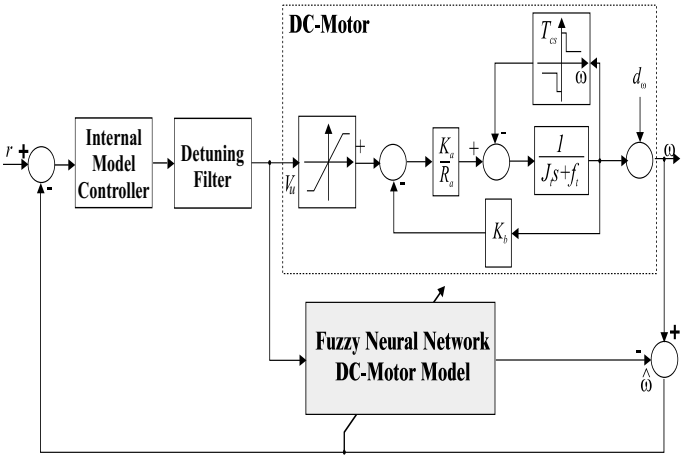

Fig. 1. Fuzzy Neural Network Internal DC–Motor Model Control Structure

This article is organized in the following manner. The material in the next section is related to the detailed modeling of the dc–motor. The following section presents the appropriate modifications of classical FNN identifiers to capture the nonlinear friction dynamics. The results from the identification of the dc–motor dynamics, and the performance of the nonlinear IMC are presented in Section IV. Conclusive remarks and the overall contributions of this work are highlighted at the last section.

II. DC–Motor System Modeling

The development of a mathematical framework for the micro- maneuvering problem of a dc–motor is addressed in this section. The commanded input to the motor results in infinitesimal low velocities. The nonlinear effects due to the imposing static friction (sticktion) need to be considered in the control compensation algorithm. The motor shaft velocity, $\omega(t)$, is detected through a tachometer sensor, and the control system is equipped with a voltage–to–voltage amplifier. To emphasize furthermore the sticktion effects, the reference angular velocity is selected to cover the four friction regimes associated with the corresponding lubrication models (static friction, boundary, partial and full lubrication regimes). However, in most typical applications, the last three terms are lumped into one, namely the full fluid lubrication regime (fflr).

The motor torque $T(t)$ is related to the applied command

voltage V_u at its terminals as shown in Figure 1

$$T(t) = J_m\dot{\omega}(t) + T_{fr}(t) = -\frac{K_aK_b}{R_a}\omega(t) + \frac{AK_aV_u(t)}{R_a} \quad (1)$$

where J_m is the effective motor inertia, K_a, R_a, K_b are the torque, armature, and the back–EMF constants respectively, A the amplifier gain, and T_{fr} corresponds to the friction torque (viscous terms are included within T_{fr}). For typical micro-maneuvering purposes the attained acceleration is close to zero ($\dot{\omega} \simeq 0$) and (1) can be modified to

$$\frac{K_aK_b}{R_a}\omega(t) = \frac{AK_a}{R_a}V_u(t) - T_{fr}(t) \ . \quad (2)$$

In this case, the dc–motor system is of zero–th order and its input–to–output relationship is sought.

Based on the definition of the static friction the dc–motor's shaft does not rotate for $|\omega(t)| \leq \omega_1$. Therefore there is a minimum voltage that needs to be provided to the motor to overcome the static friction term S_e and subsequently initiate the micro-maneuvering process. This voltage can be found from equation (2) as

$$V_u^+ = S_e\frac{R_a}{AK_a} \ . \quad (3)$$

For the fflr ($|\omega(t)| > \omega_1$), $T_{fr}(t) = b\omega + C_e\text{sign}(\omega)$ and the motor dynamics equation is

$$\omega(t) = \frac{K_aA}{bR_a + K_aK_b}V_u - \frac{R_a}{bR_a + K_aK_b}C_e\text{sign}\left(\omega(t)\right) \ . \quad (4)$$

For most practical considerations $C_e = S_e$, and the graph representing the dc–motor's simplified input/output relationship is shown in the bottom part of Figure 2. In this drawing, different values are used for: (a) the amplifier's gain A^+ (A^-) for positive (negative) applied commands, (b) the boundary values ω_1^+ (ω_1^-) for the friction lubrication regime, and (c) the static friction terms S_e^+ (S_e^-) for clockwise (counterclockwise) movements).

III. FNN–Modification for DC–Motor System Identification

The objective of the generated FNN is to capture the nonlinear characteristic of the voltage-to-angular velocity (V_u - to - ω) relationship depicted in Figure 2. The selected structure of the implemented FNN relies on the following reasoning. Assume that the following three rules are used in a very primitive FNN–approximation, as shown in the top portion of Figure 2

$$\begin{aligned} R^1 &: \text{If } V_u \text{ is } A_1 \text{ then } \omega = \beta^- \\ R^2 &: \text{If } V_u \text{ is } A_2 \text{ then } \omega = \beta^0 \\ R^3 &: \text{If } V_u \text{ is } A_3 \text{ then } \omega = \beta^+ \end{aligned}$$

where: a) the fuzzy sets $A_i, \ i = 1, 2, 3$ in the premise part are shown in the top part of Figure 2, and b) the consequence terms correspond to the slopes of the piecewise linear approximation (bottom part of Figure 2) ($\beta^- \simeq \frac{K_aA^-}{bR_a+K_aK_b}$, $\beta^0 \simeq 0$, and $\beta^+ \simeq \frac{K_aA^+}{bR_a+K_aK_b}$). The fuzzy sets $A_i, \ i = 1, 2, 3$ that appear in the premise of the FNN have membership functions (MFs) with a typical shape appearing in the top portion of Figure 2. The first (third) set attempts to capture the lubrication voltage regime $\left[V_u^{\min}, V_u^-\right]$ ($[V_u^+, V_u^{\max}]$), while the second set captures mostly the effects of the static friction regime $[V_u^-, V_u^+]$.

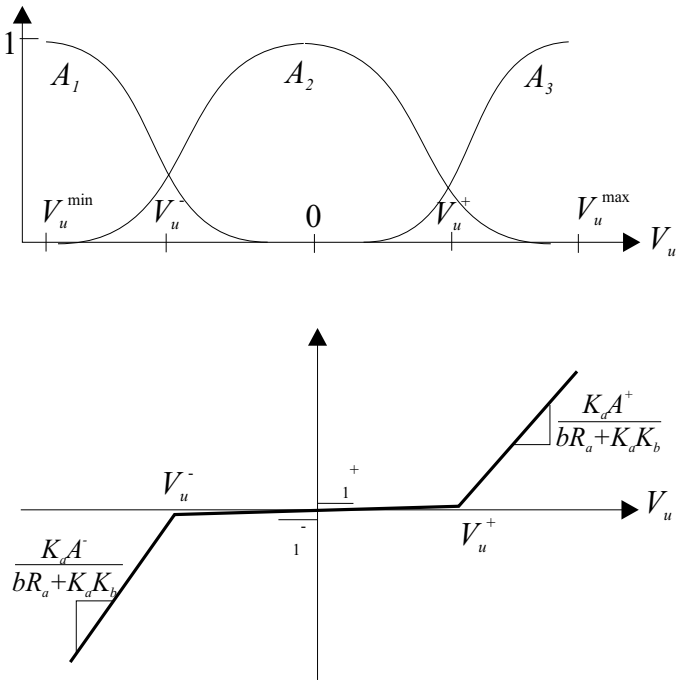

Fig. 2. Simplified Motor I/O Characteristic and MFs of the FNN–approximation

The aforementioned structure should be capable of capturing the piecewise linear approximation of the simplified motor dynamics from equation (4). However, since the friction terms are more complicated for their proper modeling division of polynomials rather than constant terms can be used in the consequence part of the FNN. Subsequently, the fuzzy rules can be modified to

$$R^d : \text{If } V_u \text{ is } A_d \text{ then } \omega = \frac{\sum_{i=0}^{n}\alpha_{d,i}\left(V_u\right)^i}{\sum_{j=0}^{m}\alpha_{d,n+1+j}\left(V_u\right)^j} \ , \quad (5)$$

where an nth (mth) order numerator (denominator) polynomial is used in the consequence part. Similarly, the number of rules can either change from $d = 3$ to a larger number to enhance the identification's accuracy, or, to a smaller number to decrease the FNN identifier's computational complexity.

The shapes of the fuzzy sets A_d in the premise are tuned in an adaptive manner, in conjuction with the terms $\alpha_{d,i}, \ i = 0, \ldots, n + m + 1$ characterizing the polynomials in the consequence part [19].

IV. FNN–IMC of DC–Motor Experimental Setup

The suggested IMC–structure was tested in experimental studies in the setup depicted in Figure 3. The used

dc–motor in this study was the E350-MGH 350-003 manufactured by ElectroCraft Corp. with parameters defined in [20,21]. A Pentium II computer (rated at 266 MHz) was used for data acquisition and control.

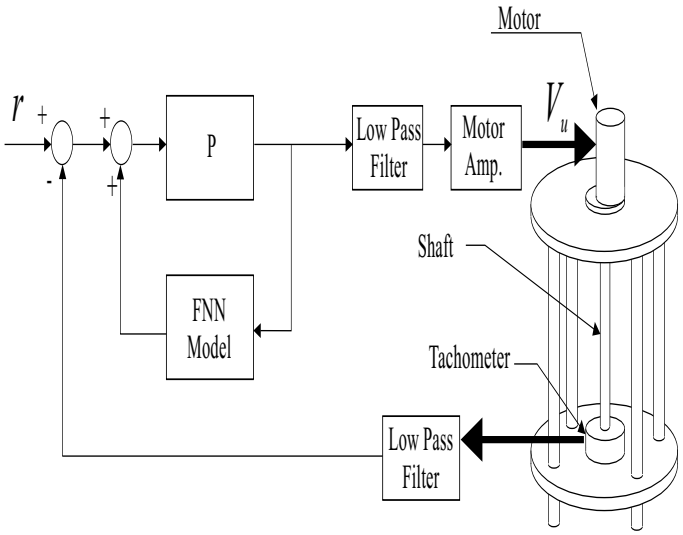

Fig. 3. DC–Motor Experimental Setup

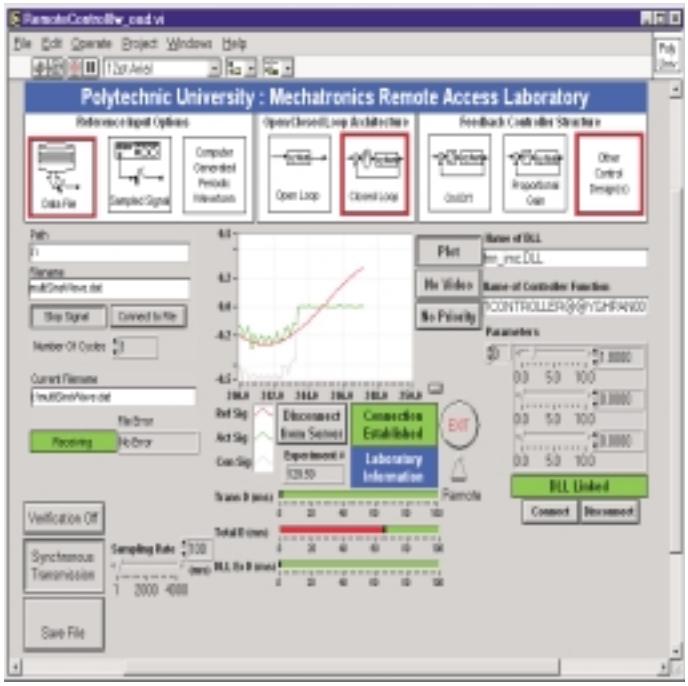

Fig. 4. IMC Virtual Instrument

The FNN–identifier was tuned off–line by exciting the system with a chirp sinusoidal signal. The typical learning CPU–time for the FNN–identifier (with 4 membership functions and 10^5–training cycles with 2,400 patterns/cycle) was 11 hours. The FNN–code was implemented in C++ and interfaced to a Labview–based front end GUI, as shown in Figure 4. Through this virtual instrument, the user can change in real–time the structure of the FNN–identifier and the feedback controller. The typical execution time for the computation of the control signal was 25 msec and the control scheme was evaluated in low sampling rates(3 to 10 Hz).

In order to investigate the validity of the assumption related to the simplified motor dynamics, the system was excited with proper signals in an open–loop configuration. The dc–motor system was excited with a sinusoidal–sweep signal to determine the input/output relationship. The utilized excitation signal $V_u(t)$ was

$$V_u(t) = \sum_{i=0}^{L} k_s \qquad \left\{ \left(t - \frac{2\pi k}{\omega_i} \right) \sin\left(\omega_i t\right) - \left(t - \frac{2\pi k}{\omega_{i-1}} \right) \sin\left(\omega_{i-1} t\right) \right\} u\left(t - \frac{1}{2\pi k \omega_i} \right),$$

where k_s is the sinusoidal amplitude, $\omega_i,\ i = 0, \ldots, L$ are the sweeping frequencies of the sinusoidal signals, k is related to the growth rate, and $u(t)$ corresponds to the step function. Figure 5 shows the motor's open-loop response for sinusoidal waves with amplitude of $k_s = 0.26$, growth rate expansion factor $k = 5$, and sweeping frequencies set at $\omega_i = 1.257,\ 0.628,\ 0.471$ and 0.314 rad/sec. The selected frequencies, amplitudes, and growth rates generate a voltage signal that forces the motor to micro-maneuver while operating within the static and lubrication friction regimes. The effects of the static friction in the system response are evident from Figure 5, where the motor does not move for $-0.28 \leq V_u \leq 0.255$ Volts. Under the assumptions stated earlier, the static input/output relationship appears in Figure 6; this waveform appears to have a similar shape to the anticipated one shown in Figure 2, and thus it is inferred that the validity of the simplified motor dynamics is credible.

A. *FNN–based DC–Motor System Identification*

The input/output (V_u and ω) data, shown in Figure 5, are used to train several FNNs. The sampling period used to record these data was $T_s = 0.1$ sec and a data stream comprised of 2,500 data points $V_u(kT_s),\ \omega(kT_s),\ k = 0, \ldots, 2499$ was used in each training cycle. The FNNs were trained in an off–line manner over a set of 100,000 repeated training cycles. Each case is defined according to the number of MFs ($A_i,\ i = 1, \ldots, d$)used in the premise part; every case is similarly separated into four sub-cases according to the order of denominator polynomial ($n = 0, \ldots, 3$ in equation (5)) used in the FNN's consequence part.

For every case, the parameters defining the MFs and the consequence terms were randomly initialized. A typical time plot ($t \in [35, 80]$ sec) of the estimated $\hat{\omega}(t)$ from the FNN model (solid line) along with the actual $\omega(t)$ (dashed–line) appears in Figure 7 for the cases where three MFs ($d = 3$) are used in the training process, the denominator polynomial corresponds to a constant ($m = 0$ in equation (5)), and the order of the numerator polynomial varies ($n = 0, 1, 2, 3$).

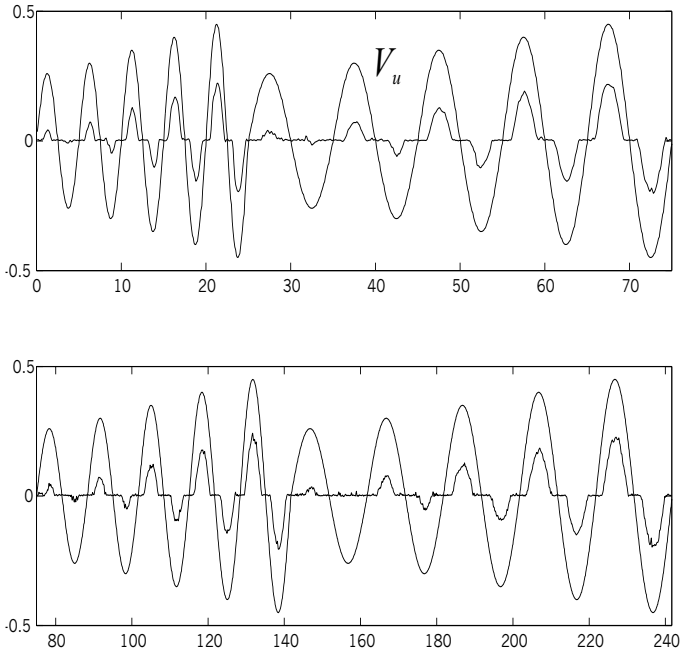

Fig. 5. Open Loop DC–Motor Response

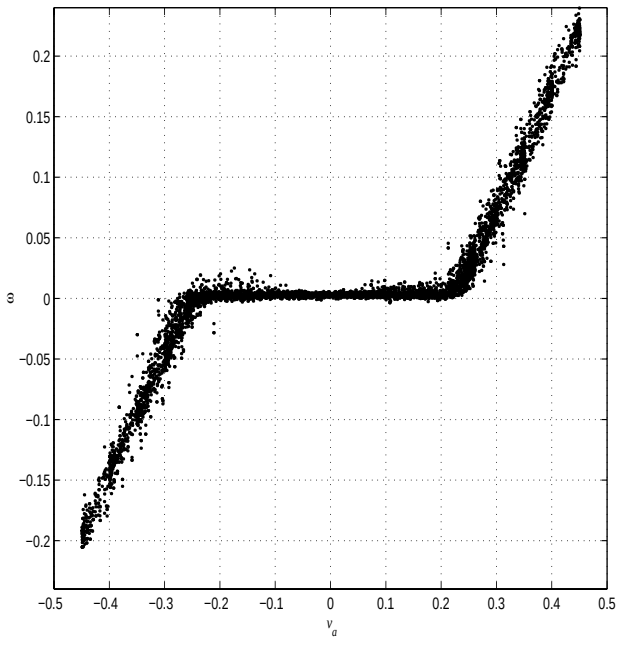

Fig. 6. DC–Motor Static Characteristic (V_u vs. ω)

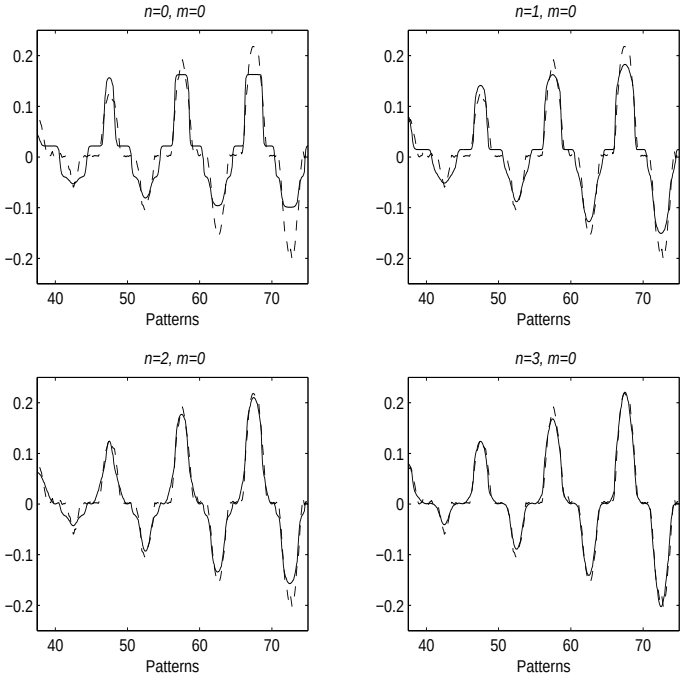

Fig. 7. Actual ($\omega(t)$) and 3MF-FNN output ($\hat{\omega}$)

B. Internal Model Control Design

The tuning of the IMC relies on the premise that the application of the FNN compensates the friction term T_{fr}. This can be achieved, under the assumption that the FNN–identifier estimates the friction characteristics and counteracts for it, as shown in Figure 1. In this case, let the nominal transfer function of the dc–motor system be

$$\omega(s) = \tilde{G}(s)V_u = \frac{AK_a}{R_a\left(sJ_m + \frac{K_a K_b}{R_a}\right)}V_u \qquad (6)$$

Accounting for the nature of the noise $\nu(t)$ corrupting the measurements and the uncertainty in the system parameters, the overall description of the friction–free linear dc–motor system is

$$\omega(t) = GV_u + \nu(t) = \tilde{G}\left(1 + l_m\Delta\right)V_u + \nu(t)\ , \qquad (7)$$

where the l_m–term characterizes the uncertainty about the nominal plant. The internal model controller, $q(e^{\jmath\omega})$, is generated by the cascade composition of: 1) an H_2 optimal controller $\tilde{q}(e^{\jmath\omega})$ for the nominal plant, and 2) a lowpass filter $F(e^{\jmath\omega})$ which detunes the controller characteristics at high frequencies in order to extend the system's robustness.

For robust performance [22], the control objective is to minimize the infinity norm of the system's weighted sensitivity function $\epsilon = 1 - Gq$, through the following $\parallel\ w_p\epsilon\ \parallel_\infty = \sup_\omega |w_p\epsilon(\jmath\omega)|$ for all members of plants $\mathcal{G} = \left\{G : |(G - \tilde{G})\tilde{G}^{-1}| \leq l_m\right\}$. The $|w_p|^{-1}$ represents an upper bound on the sensitivity function, since $|\epsilon(\jmath\omega)| \leq |w_p(\jmath\omega)|^{-1}\ \forall\omega$ if and only if $\mu = \sup_\omega\left(|\tilde{\eta}l_m| + |w_p\tilde{\epsilon}|\right) \leq 1$, where $\tilde{\eta}\ (= 1 - \tilde{\epsilon} = \tilde{G}q)$ is the complementary sensitivity function for the nominal system $\tilde{G}$.

The optimal controller design problem is formulated as

$$q = \arg\left\{\min_{q}\sup_{\omega}(|w_p\tilde{\epsilon}|+|\tilde{\eta}l_m|)\right\} = \arg\left\{\min_{q}\sup_{\omega}(|w_p(1-\tilde{G}q|+|\tilde{G}ql_m|)\right\}, \quad (8)$$

where q is the IMC feedback controller as shown in Figure 1. The efficient solution of (8) is still an active area of research. The philosophy behind the IMC–design consists of two steps, and although the resulting controller has no inherent optimality characteristics, it provides a good engineering approximation to the optimal solution of (8).

The first step amounts to designing a controller $\tilde{q}$ for good nominal performance so that

$$\tilde{q} = \arg\left\{\min_{\tilde{q}} \parallel w_p\tilde{\epsilon} \parallel_2\right\} = \arg\left\{\min_{\tilde{q}} \parallel w_p(1-\tilde{G}\tilde{q}) \parallel_2\right\}. \quad (9)$$

In this case, the optimal sensitivity becomes $\bar{\epsilon} \triangleq 1-\tilde{G}\tilde{q}$, and the optimal complementary sensitivity function $\bar{\eta} \triangleq \tilde{G}\tilde{q}$.

The second step addresses the robust stability and performance issue. At high frequencies, when the multiplicative uncertainty l_m exceeds unity, $\bar{\eta}$ has to be rolled off. To achieve this action, $\tilde{q}$ is augmented (cascaded) by a low–pass filter F, as $q \triangleq \tilde{q}F$. The order of F is such that q is proper, and its roll–off frequency is selected so that the robust stability constraint $\parallel \tilde{\eta}l_m \parallel_\infty = \parallel \tilde{G}ql_m \parallel_\infty < 1$ is satisfied. The purpose of the filter F is to detune the controller, since it sacrifices performance for robustness. This is justified since the sensitivity $\tilde{\epsilon} = 1-\tilde{G}q = 1-\tilde{G}\tilde{q}F$ (performance measure) is increased, while $\tilde{\eta} = \tilde{G}\tilde{q}F$ (robustness measure) decreases.

Since the nominal dc–motor system $\tilde{G}$ is minimum phase, the optimal solution to the minimization of the cost in (9) is independent of the weight and equal to $\tilde{q} = \tilde{G}^{-1}$. In this study, rather than assuming a first order approximation for the dc–motor system (equation (6)), its zeroeth order approximation is used. Hence, the dc–gain of the system is considered as the nominal transfer function, or $\tilde{G} = \frac{A}{K_b}$ and the nominal controller is a proportional controller with a gain of $P = \frac{K_b}{A}$.

A gain value of $P = 1.8$ was used to properly shape the complimentary sensitivity function of the linearized motor dynamics. The detuning filter was a third–order Butterworth lowpass filter with a cutoff frequency set at 20 Hz. In order to investigate the controlle's robustness against varying sampling periods, the FNN–Internal Model Proportional Controller (FNN-IMPC) was tested using various sampling periods $T_s = 100,\ 200$, and 300 msec. The utilized FNN–model is comprised of four MFs ($d = 3$) and a third order numerator polynomial ($n = 3,\ m = 0$) in its consequence portion. The experimental dc–motor responses using the FNN-IMPC are indicated in the bottom portion of Figures 8 through 10. For comparison purposes, the system's responses using only the same feedback controller (lacking the compensation FNN–term) are shown in the top portion of the same figures.

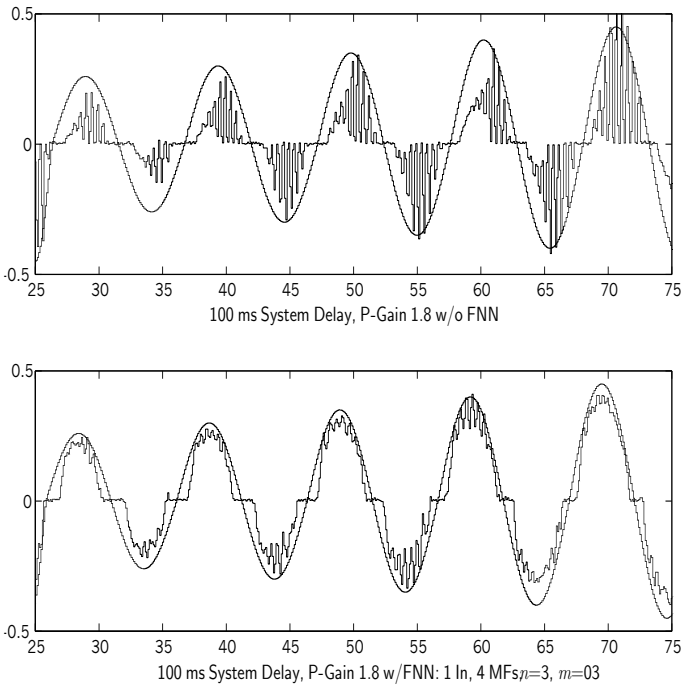

Fig. 8. DC Motor Response Using FNN-IMPC ($T_s = 10$ msec)

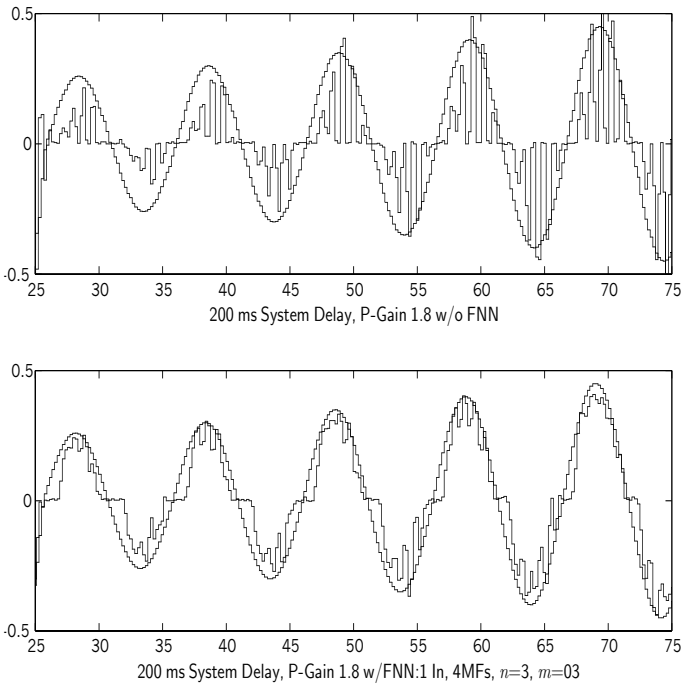

Fig. 9. DC Motor Response Using FNN-IMPC ($T_s = 20$ msec)

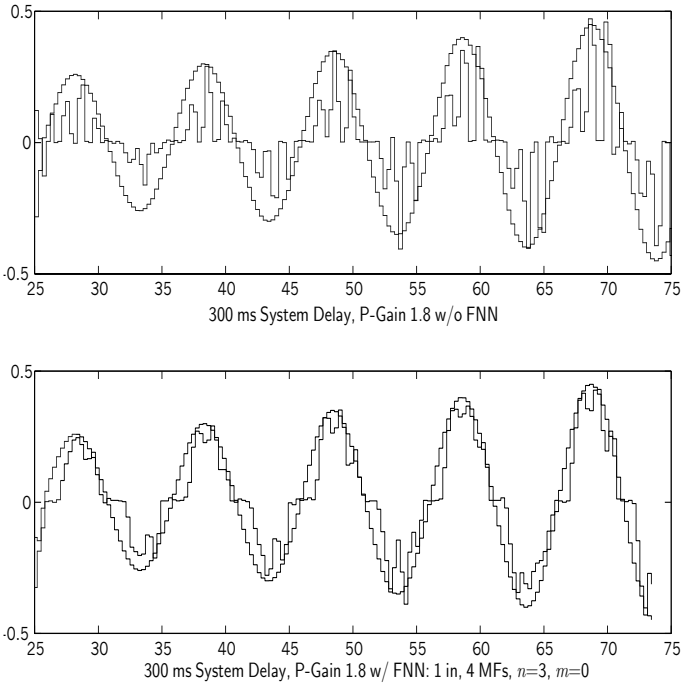

Fig. 10. DC Motor Response Using FNN-IMPC ($T_s = 30$ msec)

From the presented experimental results in Figure 8 through 10, the responses obtained with the FNN- IMPC track more accurately the sinusoidal sweeping signal than the ones attained with the P–controller. The P–controlled system's response exhibits a significant limit cycle and considerable oscillations caused by the continuous transition of the system between the static and the lubrication friction regimes. On the other hand, the FNN-IMP controlled system had notable reference– tracking capabilities at small and large sampling T_s-periods.

V. Conclusion

An internal model controller was applied for micromaneuvering purposes of a dc–motor system in this article. The controller's gain is tuned under the assumption of a system that compensates the nonllinear friction characteristics. This role is undertaken by a fuzzy neural network which identifies and subsequently compensates the friction terms. The suggsted scheme is applied in experimental studies at a prototype dc–motor system to investigate its efficiency and performance enhancement.

References

[1] J.-L. Boimond and J.-L. Ferrier, "Internal model control and max-algebra: Controller design," *IEEE Transactions on Automatic Control*, vol. 41, no. 3, pp. 457+, 1996.

[2] J. Dong and C. Brosilow, "Nonlinear IMC and PID Controller Designs," *Proceedings of the American Control Conference*, vol. 1, p. 323, 1998.

[3] M. Brown, G. Lightbody, and G. Irwin, "Nonlinear internal model control using local model networks," *IEE Proceedings-D: Control Theory and Applications*, vol. 144, no. 6, pp. 505–514, 1997.

[4] T. Lee, T. Low, A. Al-Mamun, and C. Tan, "Internal model control (IMC) approach for designing disk drive servo-controller," *IEEE Transactions on Industrial Electronics*, vol. 42, no. 3, 1995.

[5] C. Kambhampati, R. Craddock, M. Tham, and K. Warwick, "Inverting recurrent neural networks for internal model control of nonlinear systems," vol. 2, pp. 975+, 1998.

[6] Q. Li, A. Poo, and C. Lim, "Internal model structure in the control of robot manipulators," *Mechatronics: Mechanics, Electronics, Control*, vol. 6, no. 5, pp. 571+, 1996.

[7] L. Harnefors and H.-P. Nee, "Model-based current control of AC machines using the internal model control method," *IEEE Transactions on Industrial Applications*, vol. 34, no. 1, pp. 133–141, 1998.

[8] A. Tzes and P.-Y. Peng, "Fuzzy neural network control for DC-Motor micromaneuvering," *ASME Journal of Dynamic Systems, Measurement, and Control*, vol. 119, no. 2, pp. 312–315, 1997.

[9] J. Zhang and A. Morris, "Fuzzy Neural Networks for Nonlinear Systems Modelling," *IEE Proceedings-D: Control Theory and Applications*, vol. 142, no. 6, p. 551, 1995.

[10] Y. Joo, H. Hwang, K. Kim, and K. Woo, "Linguistic model identification for fuzzy systems," *Electronics Letters*, vol. 31, no. 4, pp. 330–331, 1995.

[11] C. Bor-Sen, L. Ching-Hsiang, and C. Yeong-Chan, "H^∞ tracking design of uncertain nonlinear SISO systems: Adaptive fuzzy approach," *IEEE Transactions on Fuzzy Systems*, vol. 4, no. 1, pp. 32–43, 1996.

[12] T. Dong-Ling, C. Hung-Yuan, and L. Ching-Jung, "H^∞ Control for Linear Systems with Markovian Jumping Parameters," *Control-Theory and Advanced Technology*, vol. 7, no. 2, pp. 225–229, 1999.

[13] A. Lotfi, H. Andersen, and A. Tsoi, "Matrix formulation of fuzzy rule-based systems," *IEEE Transactions on Systems, Man, and Cybernetics*, vol. 26, no. 2, pp. 332–340, 1996.

[14] C. Lin and C. Lee, "Reinforcement structure/parameter learning for neural-network-based fuzzy logic control systems," *IEEE Transactions on Fuzzy Systems*, vol. 2, no. 1, pp. 46–63, 1994.

[15] R.-N. Singh and W. Bailey, "Fuzzy logic applications to multisensor-multitarget correlation," *IEEE Transactions on Aerospace and Electronics Systems*, vol. 33, no. 3, pp. 752–769, 1997.

[16] S.-J. Huang and R.-J. Lian, "A hybrid fuzzy logic and neural network algorithm for robot motion control," *IEEE Transactions on Industrial Electronics*, vol. 44, no. 3, pp. 408+, 1997.

[17] R. King, "Artificial neural networks and computational intelligence," *IEEE Computer Applications in Power*, vol. 11, no. 4, pp. 14–25, 1998.

[18] S. Weerasooriya and M. A. El-Sharkawi, "Laboratory implementation of a neural network trajectory controller for a dc motor," *IEEE Transactions on Energy Conversion*, vol. 8, no. 1, 1993.

[19] J. Overstreet, "Remote monitoring and advanced control designs for internet–based experimentation," Master's thesis, Polytechnic University, Mechanical Engineering Department, 2000.

[20] A. Tzes, P.-Y. Peng, and C.-C. Houng, "Neural Network Control for DC–Motor Micromaneuvering," *IEEE Transactions on Industrial Electronics*, vol. 42, pp. 516–523, Oct. 1995.

[21] A. Tzes, P.-Y. Peng, and J. Guthy, "Genetic–based Fuzzy Clustering for DC–motor Friction Identification and Compensation," *IEEE Trans. on Control Systems Technology*, 1997.

[22] M. Morari and E. Zafiriou, *Robust Process Control*. Englewood Cliffs, NJ: Prentice-Hall, 1989.